International Journal of Latest Research in Engineering and Technology (IJLRET)
ISSN: 2454-5031
www.ijlret.com || Volume 11 - Issue 11 || November 2025 || PP. 52-58

Synthesis of ZnO Nanoparticles by Chemical Methods for Photo Detector Applications

Surour A. Khlaf
Ministry of Education, Al-Karkh 3, Al-Fatemiyyat Intermediate School

Abstract: This paper involved the synthesis and characterisation of Zinc Oxide (ZnO) nanoparticles and the analysis of their structure and optical characteristics, and one of their potential applications in Photodetectors.ZnO nanoparticles were prepared by a simple chemical procedure (chemical precipitation) which included the use of aqueous zinc nitrate and sodium hydroxide and then drying at 200 Celsius. Structural and Morphological Characterization X-ray Diffraction (XRD). The structural characterization confirmed the proper formation of Zinc Oxide crystals in the hexagonal crystalline phase (Wurtzite). The crystallite size was estimated between 5.65 nm and 12.52 nm which proves the nano-scale nature of the material. Atomic Force Microscopy (AFM) and Field Emission Scanning Electron Microscopy (FESEM). The obtained results indicated a rough and granular surface morphology, and size of the large nanorods or nanowires fell between 2-5 µm long and the width measured in the nanometer range. FTIR verified the existence of the characteristic Zn-O bond, further confirming the nanocrystalline nature of the material. Optical Investigations and Quantum Confinement Effect Optical analysis (UV-Vis) revealed that the optical band gap of the prepared material is 3.43 ev electron volts (eV). This is a bulk Zinc Oxide value band gap that is about 3.37 eV. This high band gap is being regarded as a decisive confirmation of the Quantum Confinement Effect, and it proved the achievement of the formation of nanostructures with quantum-confined dimensions. The material had spectral characteristics of the wide-bandgap semiconductors, which are highly sensitive in the Ultraviolet (UV) region and have high transparency in the visible spectrum. These properties render the material a viable solution in the next generation of applications on Ultraviolet Photodetectors (UV Photodetectors) and transparent electronics.
Keywords: zinc oxide (ZnO), Wide energy gap, Optical properties, Spectral response, XRD, FTIR.

1. Introduction

ZnO is an inorganic material, a compound of physical properties that is useful in electronics, optics and material science. It usually crystalizes in the wurtzite (hexagonal) structure, making it possess special optical, electrical and piezoelectric properties. ZnO is a wide-band-gap semiconductor (≈3.3 eV at room temperature), enabling strong UB absorption as well as visible-range transparency. It appears as a white crystalline powder, with density of approximately 5.6 g/cm³with high thermal stability with melting point of more than 1975 Celsius [2].

Also, ZnO has significant piezoelectric and pyroelectric characteristics as it has a non-centrosymmetric crystal structure, and therefore it can be used in sensors, actuators, and energy-harvesting devices [3]. With its UV absorption, thermal stability, high electronic mobility, and chemical strength, ZnO has become a key component in the diverse array of technologies, such as sunscreens, transparent electronics, varistors, semiconductor components [4]. Some research works were dedicated to the parameters which influenced the particle size of ZnO using the PLD method.

Desorption [5], nucleation, substrate surface roughness, adsorption, crystallization/re-crystallization, surface diffusion, also morphology of deposited ZnO thin films are examples of thermally activated deposition characteristics that can be controlled by a number of variables such as: substrate temperature, background gas pressure [6], repetition rate, laser energy density (i.e., laser impact) oxygen partial pressure in the deposition chamber, target-to-substrate distance, thickness of ZnO thin films formed resulting in different property modifications [7], also post-growth annealing. Controlling the morphological, optical, along with structural properties of ZnO films is largely dependent on film thickness. The deposited ZnO thin films are thicker when the deposition period is longer [8].

2. Experimental

Zinc nanoparticles were prepared using zinc nitrate hydrate 2.9g (Zinc NITRATEH exahydrate 99%, LOBA ChemiE PVT. LTD, M.W.297.49) per 100 ml of deionized water. The zinc nitrate hydrate was dissolved at a temperature below 50°C for 1 hour until it became completely transparent, i.e., at a molar concentration of 0.1M. Then, 2 g of sodium hydroxide has been prepared through dissolving in 50 ml of deionized water with continuous stirring for 10 minutes. After adding another mL of sodium hydroxide to the zinc nitrate hydrate, a

reaction was observed, forming a white precipitate of zinc oxide at the bottom of the beaker. After separating the salt water from this precipitate and drying it at 200°C for 2 hours, zinc nanoparticle powder was obtained.

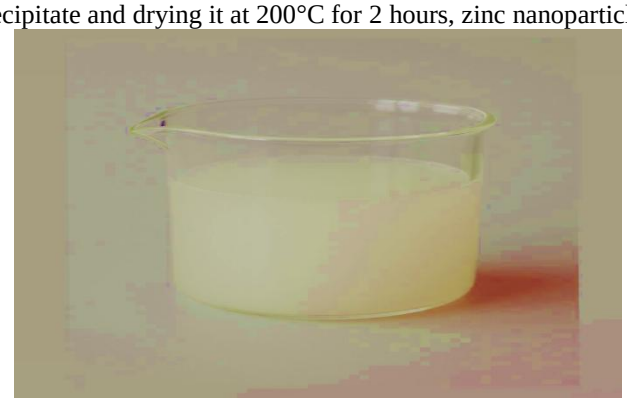

Fig.1: ZnO freshly colloidal nanoparticles which are prepared by chemical

3. Results and discussion

XRD pattern regarding the prepared ZnO sample is presented in Figure (2) ،where the diffracted intensity (counts) is plotted as a function of the Bragg angle 2\theta.

Measurements have been performed with the use of Cu-Kα radiation (\lambda = 1.5406 Å). In addition, the diffraction profile shows many characteristic features providing insight into the structural properties, crystallinity, as well as phase composition regarding the sample.The pattern indicates the existence of multiple diffraction peaks within range 2\theta = 10^\circ – 40^\circ, corresponding to crystallographic planes often related to the hexagonal wurtzite structure of ZnO (JCPDS Card No. 36-1451).

The formation of crystalline ZnO is supported by the appearance of these peaks. Also, it can be seen that some of the reflections have become broad, indicating the existence of nanoscale crystallites and/or internal lattice strain in the structure, as has been observed by[9]. The background intensity is relatively high, particularly at smaller angles of diffraction, over the entire pattern. Such an increase in the intensity of the baseline suggests the existence of an amorphous component in the sample or a large amount of diffuse scattering that is attributed to surface roughness or residual precursor materials. These are similar characteristics that have been observed in ZnO materials synthesized [10].

Moreover, the pattern has several small peaks distributed across the scan range. The presence of secondary phases or structural inhomogeneities in trace amounts may be manifested in these peaks. Although their intensity is low, their distribution indicates that the sample is not phase-pure. Pearton et al. (2005) explain that these extra peaks are usually caused by incomplete conversion of precursors or formation of mixed zinc-oxygen species during the synthesis.

The gradual reduction of the intensity of the diffraction beyond2\theta \approx 40^\circ shows the lack of the high order reflections and this indicates that the predominant crystal type is the ZnO. The overall diffraction profile, which is a set of recognizable ZnO peaks over a fairly high background, confirms that the sample is a mixture of crystalline ZnO and an amorphous component, which is expected of chemically synthesized oxide materials.

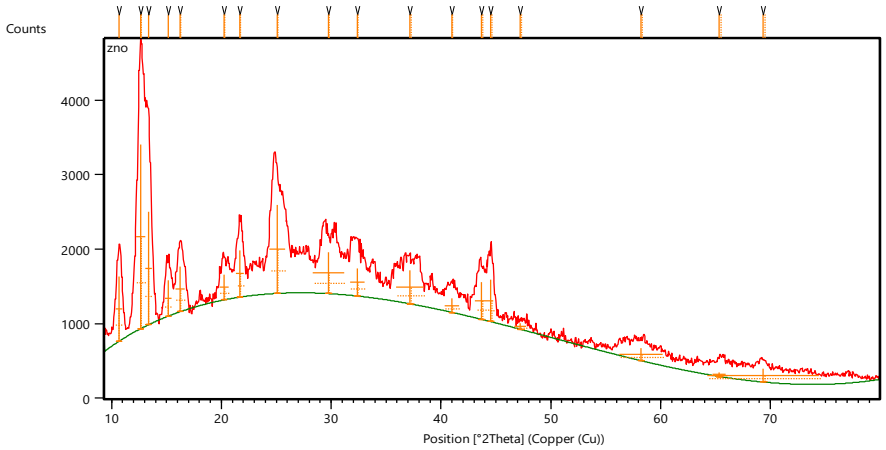

Figure (2): ZnO thin-film XRD anlysise

The crystallite size (D) has been calculated with the use of Scheerer's formula [11].

$$D = \frac{0.9Y}{\beta C o S \theta} \quad \ldots\ldots\ldots\ldots\ldots\ldots (1)$$

Table (1): X-Ray characterization for ZnO

2Θ (deg)	(hkl) planes	B (deg)	D (nm)
15.150	(200)	0.64	12.52
25.134	(101)	1.44	5.65
31.7	(100)	1.31	6.32

AFM results he accompanying image is a 3D topography of a material's surface, obtained using atomic force microscopy (AFM). [1[The surface exhibits high roughness and a distinct granular nature. The material consists of numerous irregularly arranged grains or crystallite.The color contrast (from dark orange to light yellow) indicates the variation in vertical height (Z-axis). The lighter (yellow) areas represent the grain peaks or highest points on the surface, while the darker (orange/brown) areas represent the valleys or lowest points.Roughness Scale:Z-axis shows that the difference between the lowest point (0.0 nm) and the highest point (7.9 nm) on the surface is 7.9 nm. This extremely small range confirms that the measurement is at the nanoscale.

The significant difference in the heights within the 7.9 nm range across an area demonstrates that the surface is not smooth. The image depicts a rough, granular nanoscale surface, which is typical of thin films that are produced by deposition processes. The topmost height (7.9 nm) indicates that the material does not have much roughness in the absolute scale, but the nanoscale roughness is crucial in the conditions of the material and its use.

The shape of the fitting curve suggests that the distribution is closer to the log-normal distribution in that the surface growth changes are gradual. The findings confirm that the surface possesses low roughness and reasonable uniformity, thus it can be used in application where there is need of stable topographic characteristics.

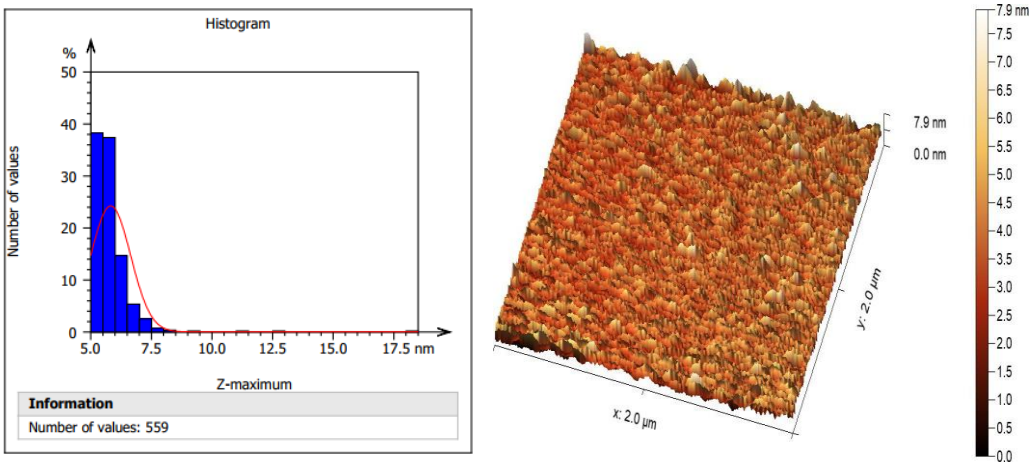

Fig.3: 3D AFM images ofZnO surface and Granularity accumulation distribution chart.

ZnO NPs FTIR spectra revealed multiple significant absorption peaks. Zn–O stretching vibration mode is responsible for the broad absorption band in (500–4500) cm−1 region; the sample's nanocrystalline structure is shown by the absorption band's broadness. The samples utilized in the presented investigation were substantially smaller compared to ZnO bulks. The graph represents ZnO FTIR spectrum. The strong peak in low wave number region (less than 600 cm^{-1}), which indicates the tension vibration regarding Zn-O bond, is the key peak verifying the material's structure. Other peaks at roughly 1630 cm^{-1} and 3400 cm^{-1} show that water molecules and/or hydroxyl groups (-OH) have been absorbed on the surface of ZnO particles, which is a typical occurrence in prepared nanomaterials.

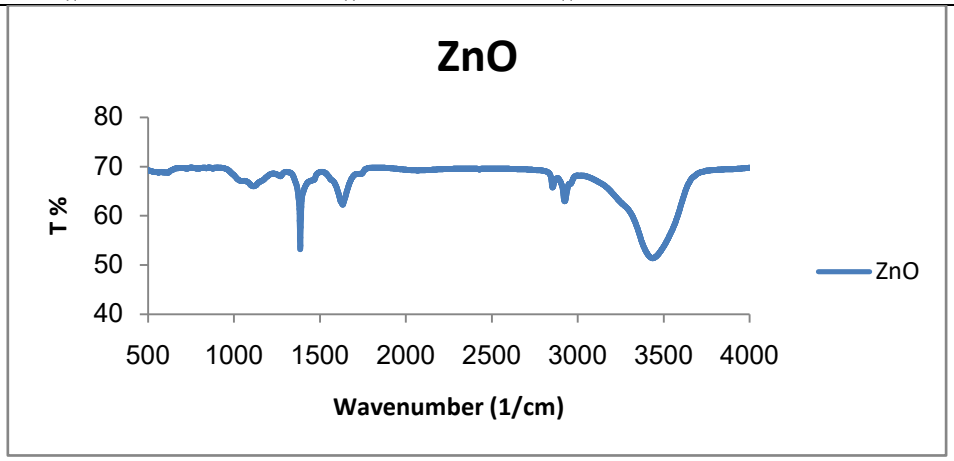

Fig.4: FTIR spectra ZnO of thin film as a function of wave number

FESEM was used to study ZnO nano thin films morphology. The image shows large-scale nanorods or nanowires Obe is a very frequent crystalline form of zinc oxide due to its crystalline nature Scale in the image = 5 μmThe average length of the lines is clearly ≈ 2–5 μm The greatest variation is between ≈ 50–150 nm Smooth surface alternatives indicate Good crystal growth (high crystallinity Reduced impurities during growth).

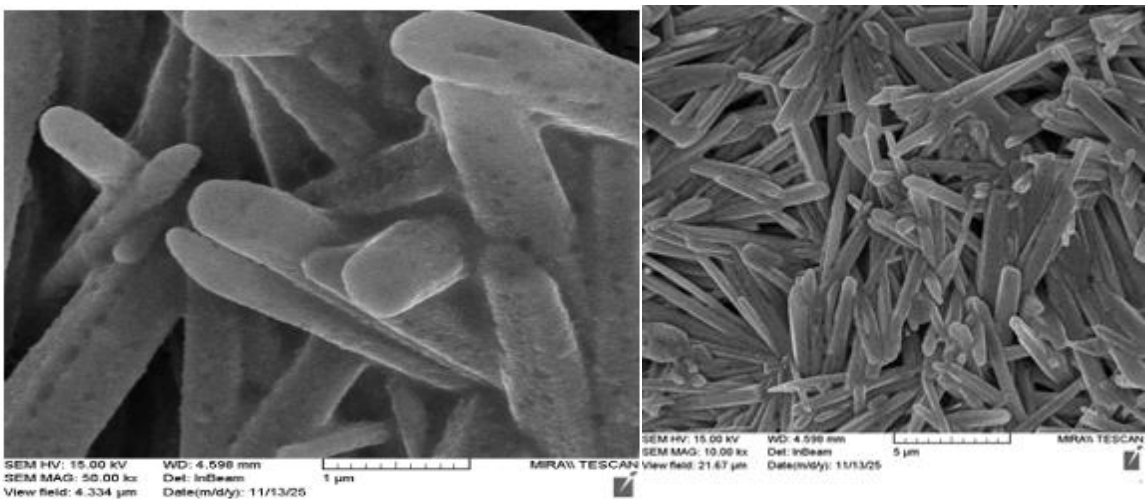

Figure 5: FESEM images of ZnO nano-thin films

The transmittance spectrum regarding ZnO thin film is displayed in Fig 6. In UV region, the data are adjusted for glass transmission. Additionally, the figure indicates that the absorption edge's transmission spectra are located at about 378 nm. The unique optical characteristics related to nano-semiconductor materials are illustrated by the findings of the examination regarding UV-Vis spectroscopy data for ZnO samples. The quantum confinement effect is clearly demonstrated by the high optical energy gap value (Eg = 3.974 eV) in comparison to the bulk value regarding ZnO (approximately 3.37 eV) [12].

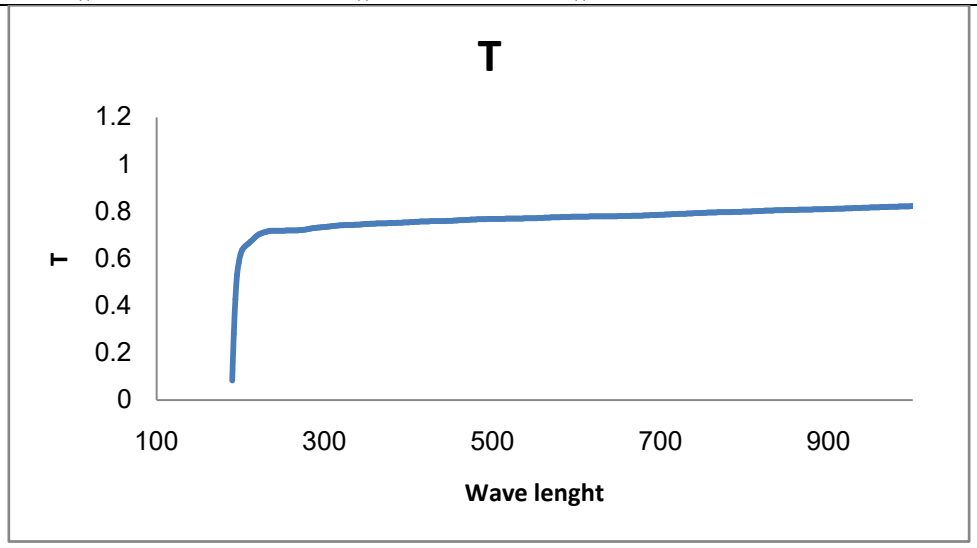

Fig. 6: Transmittance spectrum of (ZnO) thin film.

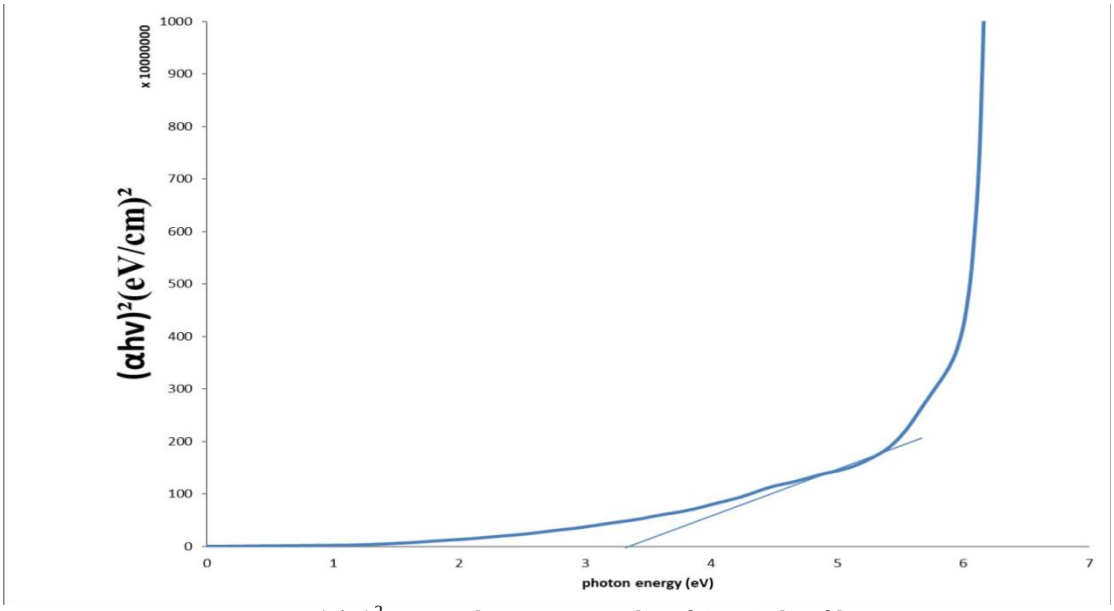

Fig.7: $(\alpha hv)^2$ versus photon energy plot of (ZnO) thin film

Consequently, the absorbance (A) is defended as logarithm (base 10) regarding the reciprocal of transmittance utilizing the basic relation between photon transmission as well as absorbance [13]:

$A = \text{Log}\frac{1}{T}$…….. (2)

In the case when A is (ZnO) thin film's absorbance and T is its transmittance. Relations were used to find the film's reflection [14]:

R + T+ A =1 ……(3)

Fig (7) shows that the optical absorption coefficient α has been assessed with the use of tauc relation α hv = A (hv - E_g)^n in which *α=2.303 A/t where t* represent film thickness, *hv* represent the photon energy, and *n* = 1represent allowed direct transition[15]. From Plotting graph between $(\alpha hv)^2$ versus photon energy *(hv)* gives the value of direct band gap. The extrapolation of the straight line to $(\alpha hv)^2 = 0$, gives the value of band gap, shown in figure7.The optical band gap is 3.34 eV, in other word, the exactions wavelength ~378nm.

Spectral response is an important parameter for photonic or stereoscopic detectors,· The curve shows that the response starts low at a wavelength of 350 nm (blue end / UV), then increases rapidly to reach a peak of around 550 nm (the green area of the visible spectrum), then gradually decreases as the wavelength increases to almost zero at 850 nm near infrared terminal) Interpretation of form and peak ·Peak around 550 nm: corresponds to the area of extreme sensitivity to the human eye (green light). This suggests that the sensor is designed to be optimal in the visible area, and may be used in applications such as cameras or photometers.Decrease in the blue region (350-450 nm): may be due to lower absorption of high-energy (short-wave) photons in the semiconductor material used (such as silicon), or due to the presence of blue/UV light obserbation layers.The decrease in the red and infrared region (650-850 nm): occurs because the photons of this region with low energy may not be sufficient to bypass the gap energy barrier (Bandgap) of the material.

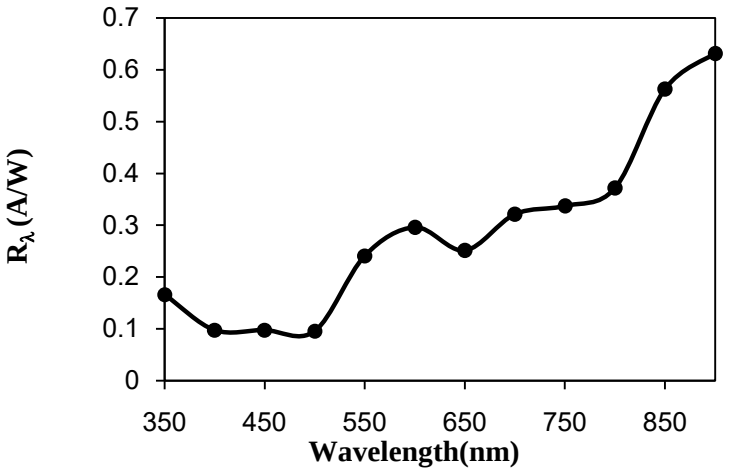

Figure 8 | Spectral characterization of the photodetectors Spectral response of ZnO

Figure (9) he specific detectivity (D*) spectrum of the ZnO-based photodetector exhibits a wavelength-dependent response governed by the intrinsic band structure and defect-related electronic transitions within the material. In the ultraviolet region (≈350–400 nm), D* decreases despite strong optical absorption, primarily due to the rapid recombination of photogenerated carriers, which limits the net photocurrent. In the visible range (450–700 nm), the detectivity remains relatively low and fluctuating, reflecting the sub-bandgap absorption arising from intrinsic point defects such as oxygen vacancies (V_O) and zinc interstitials (Zn_i), which contribute weakly to carrier generation.

At longer wave lengths (700–850 nm), a pronounced increase in D* is observed. This enhancement is attributed to deep-level defect states that prolong carrier lifetime and improve the signal-to-noise ratio, thereby elevating the detector performance even in the sub-bandgap region where direct interband transitions are forbidden. Overall, the spectral behavior of D* indicates the combined influence of band-edge absorption, defect-mediated transitions, and noise characteristics inherent to ZnO nanostructures.

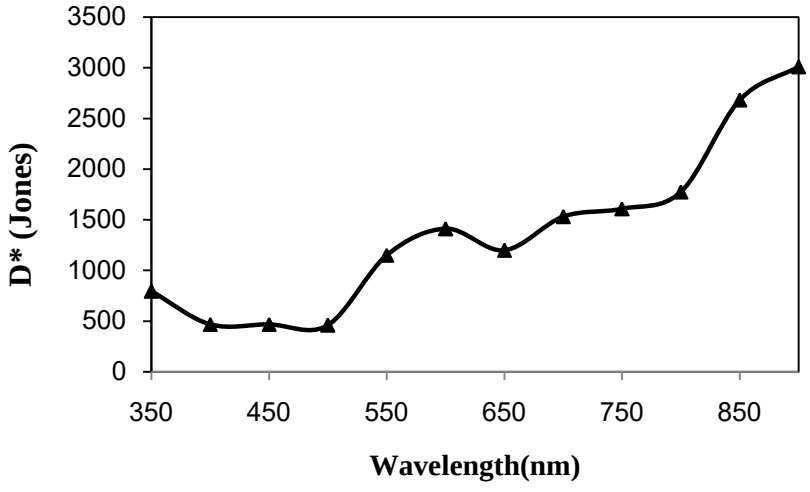

Figure 9 | Spectral characterization of the photo detectors Specific Detectionivity of ZnO

4. Conclusion:

The ZnO material synthesized is able to support the creation of a successful formation of the nanocrystalline structure with a well-defined physical and optical properties. The XRD structure analysis identified the hexagonal crystal phase of wurtzite in the material (JCPDS Card No. 36-1451). The generality in terms of diffraction peaks and estimated crystallite sizes that are between approximately 5.65 nm to 12.52 nm is in tandem with the nanoscale characteristics of materials.

This conclusion was corroborated through morphological studies, which showed a surface with rough, granular topography (AFM) as well as the presence of large-scale nanowires or nanorods (FESEM) with micrometer-long and nanometer-wide widths. The distinctive Zn-O stretching vibration mode was used by FTIR to establish the chemical composition, and the wide absorption band supported the nanocrystalline condition. Importantly, the optical study demonstrated the quantum confinement effect through clear physical evidence.

The analysis compares the optical band gap calculated to be blue-shifted when compared to bulk ZnO value. This is a key physical impact of the reduced particle size that proves the successful synthesis when it comes to quantum-confined ZnO nanostructures. The material can be used as a prospective material in UV photodetectors and in transparent electronics since its spectral characteristics to its high detectivity in the UV region and great transparency in visible spectrum are spectral properties compatible with wide-gap semiconductor.

References

[1]. Haynes, W. M. (2020). CRC Handbook of Chemistry and Physics (100th ed.). CRC Press.
[2]. Özgür, Ü., Alivov, Y. I., Liu, C., et al. (2005). “A comprehensive review of ZnO materials and devices.” Journal of Applied Physics, 98(4), 041301.
[3]. Klingshirn, C. (2007). “ZnO: Material, physics and applications.” Chem Phys Chem, 8(6), 782–803.
[4]. Soci, C., et al. (2010). “ZnO nanowire UV photodetectors.” Journal of Nanoscience and Nanotechnology, 10(3), 1430–1449.
[5]. M. S. Al-Assiri, M. M. Mostafa, M. A. Ali, and M. M. El-Desoky, "Optical Properties of Annealed ZnO Thin Films Fabricated by Pulsed Laser Deposition," *Silicon*, vol. 7, 2015.
[6]. Camelia Popescu, Gabriela Dorcioman, and Andrei C. Popescu, "Laser Ablation Applied for Synthesis of Thin Films: Insights into Laser Deposition Methods," in *Applications of Laser blation*, Intech Open, 2016, pp. 3-32.
[7]. Rajesh Kumar, Girish Kumar, and Ahmad Umar, "Pulse Laser Deposited Nanostructured ZnO Thin Films: A Review," *Journal of Nanoscience and Nanotechnology*, vol. 14, p. 1911–1930, 2014.
[8]. Jae-Min MYOUNG, Wook-Hi YOON, Dong-Hi LEE, Ilgu YUN, Sang-Hyuck BAE, and SangYeol LEE, "Effects of Thickness Variation on Properties of ZnO Thin Films Grown by Pulsed Laser," *Jpn. J. Appl. Phys.*,vol. 41, p. 28–31, 2002
[9]. Özgür Ü., Alivov, Y. I., Liu, C., et al. (2005). A comprehensive review of ZnO materials and devices. Journal of Applied Physics, 98(4), 041301.
[10]. Klingshirn, C. (2007). ZnO: Material, physics and applications. Chem Phys Chem, 8(6), 782–803
[11]. E. Kashevsky, V.E. Agabekov, S.B. Kashevsky, K.A. Kekalo, E.Y. Manina, I.V. Prokhorov, V.S. Ulashchik, *Particuology*6 (2008) 322
[12]. Samanta, P. K. (2020). Band gap engineering, quantum confinement, defect and surface states in ZnO nanostructures. Optical Materials, 108, 110175.
[13]. N. Bala Sundaram and V. Veeravazhuthi, "Thin Film Techniques and Applications", Allied Publisher PVT Limited, New Delhi, (2004).
[14]. S. A. Tawfiq "A study of optical and electrical properties of the cadmium stannate material using the Co - Evaporation method"PH.D. Thesis, Al –Mustansiriya University, (1996)
[15]. Y. Sirotin, Y. M. Shaskolskaya "Fundamentals of crystal physics ", Mir Publishers, Moscow, (1982).